A polarized neutron study of some $Co_{1-x}Mn_x$ alloys

1992 J. Phys.: Condens. Matter 4 8961

(http://iopscience.iop.org/0953-8984/4/46/003)

J. Phys.: Condens. Matter 4 (1992) 8961–8968. Printed in the UK

A polarized neutron study of some $Co_{1-x}Mn_x$ alloys

A R Wildes†, S J Kennedy‡, L D Cussen§ and T J Hicks†

† Department of Physics, Monash University, Clayton, Victoria 3168, Australia
‡ Australian Institute of Nuclear Science and Engineering, Private Mailbag 1, Menai, NSW 2234, Australia
§ Department of Applied Physics, Victoria University of Technology, PO Box 64, Footscray, Victoria 3011, Australia

Received 18 June 1992

Abstract. Samples of $Co_{68}Mn_{32}$ and $Co_{63}Mn_{37}$ were examined with neutron polarization analysis over a scattering vector range that encompasses the first Brillouin zone in the FCC structure. The atomic disorder cross section was separated and fitted for short-range-order Cowley parameters, and the magnetic cross section was separated. The magnetic cross sections could be satisfactorily compared with those calculated for zero scattering vector from previous susceptibilty measurements using the quasistatic approximation. However, the scattering vector dependence of the magnetic cross section is quite different to that expected from a localized moment model, and indicates that the average moment per atom is small.

1. Introduction

Past magnetic studies of $Co_{1-x}Mn_x$ alloys have shown curious phenonmena at low Mn concentrations, in particular the region $25 < x < 42$ (Kouvel 1960, Rhiger *et al* 1980). For $x < 25$ the magnetic phase diagram for this system (Men'shikov *et al* 1985) shows the alloy to be ferromagnetic with a Curie temperature that steadily decreases with increasing Mn concentration; however, the transition between this phase and the antiferromagnetic phase (clearly measured for $x > 42$) is not a simple one.

Paramagnetic and antiferromagnetic clustering, quoted as existing in this region, promised interesting magnetic short-range-order studies. The ability of neutron polarization analysis to distinguish between magnetic and atomic order made this the perfect tool to examine the short-range order in these samples.

Past studies using polarized neutrons have been made on these alloys in the range $x < 25$ (Cable 1982) to measure the magnetic short-range order in the ferromagnetic phase. These studies revealed a moment disturbance function decreasing in magnitude with increasing Mn concentration, and from this Cable was able to calculate, using the Marshall model of magnetic defects in ordered magnets (Marshall 1968), the average ferromagnetic moments on the Co and Mn atoms. These moments were shown to decrease with Mn concentration, and in extrapolation would appear to approach zero near 30 at.% Mn.

Kouvel (1960), in a comprehensive early investigation of this composition range, observed displaced hysteresis loops after cooling in a field, and measured the ferromagnetic and paramagnetic moments for different compositions. The latter were

0953-8984/92/468961+08$07.50

average moments taken from the Curie constant at high temperatures. According to this work, the ferromagnetic moment goes to zero near 30 at.% Mn, but in contrast the paramagnetic moment steadily increases with increasing Mn concentration. We thus expected to see a very large magnetic cross section appear in the paramagnetic phase.

2. The specimens

Specimens of $Co_{1-x}Mn_x$ were prepared by firstly taking 99.99% purity Mn and 99.999% purity Co and melting them under purified argon in an induction furnace. The fused mix was then cut and remelted a number of times in an argon arc furnace, and finally the samples were homogenized by annealing them, again under argon, at 1000 °C for a week before quenching them in water. The final samples were swaged into cylinders of 10 mm diameter, and cut to give 30 mm lengths. Their composition was checked using an electron microprobe.

Two samples were examined, with 37 at.% and 32 at.% Mn. Due to the high absorption cross section and the null-matrix characteristics of the alloys, the 30 mm rod were spark cut to give an annular cross section, the wall thickness calculated to give a $1/e$ transmission. The samples were then annealed at 1000 °C for 15 h and quenched in water. The structure was examined using x-ray diffraction, and shown to be FCC with $a_0 = 3.59$ Å.

3. Experiment

The experiments were performed on the LONGPOL polarization analysis neutron spectrometer at the HIFAR facility. The instrument makes use of monochromatic neutrons of wavelength 3.6 Å that then pass through a magnetized iron polarizing filter. A neutron spin flipper before the sample position was used, and the subsequent neturon polarization after scattering by the sample was analysed once again by magnetized iron filters. The instrument has eight detectors, and a mean net polarization of approximately 37% was obtained in each detector. Temperature control down to 20 K was achieved using a helium cryorefrigerator.

Two types of measurement were made on LONGPOL. The first was a time-of-flight-style measurement made by alternately turning the spin flipper on and off by means of a pseudo-random pulse (Cussen *et al* 1992). The second was simple flipper-on and flipper-off measurements to find the spin-flip and non-spin-flip cross sections.

The experiments were carried out with the neutron polarization perpendicular to the scattering vector. This means that one half of the magnetic cross section is in the spin-flip cross section, and the other half is in the non-spin-flip cross section, i.e.

$$\sigma_{nsf} = \sigma_d + \tfrac{1}{3}\sigma_i + \tfrac{1}{2}\sigma_m \qquad \sigma_{sf} = \tfrac{2}{3}\sigma_i + \tfrac{1}{2}\sigma_m$$

where σ_{sf} is the spin-flip cross section, σ_{nsf} is the non-spin-flip cross section, σ_i is the nuclear spin incoherent cross section, σ_d is the atomic disorder cross section which contains the atomic short-range order, and σ_m is the magnetic cross section.

A more desirable configuration would be with the polarization parallel to the scattering vector, in which case the magnetic cross section would appear entirely in

the spin-flip cross section, and the atomic disorder cross section entirely in the non-spin-flip cross section. Unfortunately, as the LONGPOL spectrometer is currently being redeveloped, this facility is not yet available.

For the purposes of background subtraction the samples were carefully attenuation matched with an indium sample of approximately the same geometry. Indium has a high absorption cross section and low scattering cross sections, thus it was ideal for use as a non-scattering 'blank' to measure background. A count-time ratio of 3:1 was maintained between the sample and the indium. Careful background subtraction was particularly necessary for these alloys because of the high Co absorption and consequent small scattered intensity.

Because it is quoted in the literature as a clustering antiferromagnet (Men'shikov *et al* 1985), measurements were taken on $Co_{63}Mn_{37}$ at three temperatures: room temperature, 150 K, and 20 K. Similarly, as it is quoted as being a paramagnet to absolute zero, $Co_{68}Mn_{32}$ was measured only at 30 K. On each sample a 24 h time-of-flight-style measurement was made to check for any non-magnetic inelastic scattering. Static flipper-on and flipper-off measurements were then taken, and the raw counts collected and analysed. The (100) position for the FCC phase of these alloys appears at $\kappa \approx 1.75$ Å^{-1} and thus measurements were taken up to $\kappa \approx 2.5$ Å^{-1} in order to safely encompass the first Brillouin zone.

Relative detector dffciency and polarization calibration were measured by repeating the experiments substituting a vanadium sample of similar geometry. Multiple-scattering and true absorption corrections for the vanadium data were made by the techniques of Blech and Averbach (1965), Harders *et al* (1985), and Bally *et al* (1964). Absolute cross sections for the data could then be calculated. It is worth mentioning here that due to the high absorption cross section of the $Co_{1-x}Mn_x$ samples, multiple scattering from these samples could be safely ignored.

The analysed data could then be fitted for atomic short-range order using a non-linear least-squares fitting routine to determine Cowley parameters, and any magnetic structure could subsequently be determined.

4. Discussion

The first and perhaps the most surprising observation made was that there appears to be no change in the cross section of $Co_{63}Mn_{37}$ with temperature (see figure 1). This concentration has been quoted as being a clustered antiferromagnet (Men'shikov *et al* 1985). Thus we were expecting to see a large temperature dependent magnetic short-range order. This is notably absent. We therefore felt justified in averaging the data from all three temperatures and working with these cross sections.

There was, however, some non-temperature-dependent structure in both samples. By subtracting the spin-flip from the non-spin-flip cross sections the atomic disorder cross section could be isolated. The function used to fit this cross section (see figure 2) was

$$\left(\frac{d\sigma}{d\Omega}\right)_d - \frac{1}{3}\left(\frac{d\sigma}{d\Omega}\right)_i = c(1-c)(b_{Co} - b_{Mn})^2\left\{\alpha_0 + \sum_{R_n} \alpha_n \frac{\sin(\kappa R_n)}{\kappa R_n}\right\}$$

using $(d\sigma/d\Omega)_i$ as the nuclear spin incoherent cross section and α_n as the Cowley short-range order parameters shown in table 1.

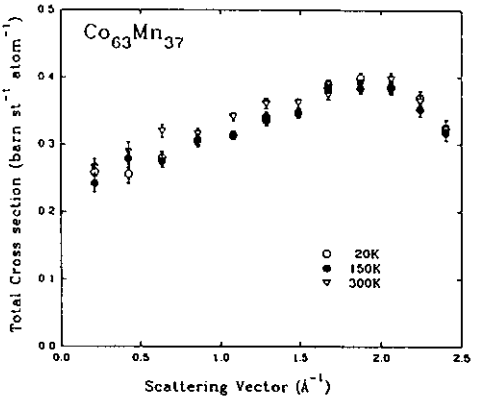

Figure 1. The total cross section of $Co_{63}Mn_{37}$ at the temperatures measured. The spin-flip and non-spin-flip cross sections at each temperature were separated from these data, and there was no difference between temperatures observed for these cross sections.

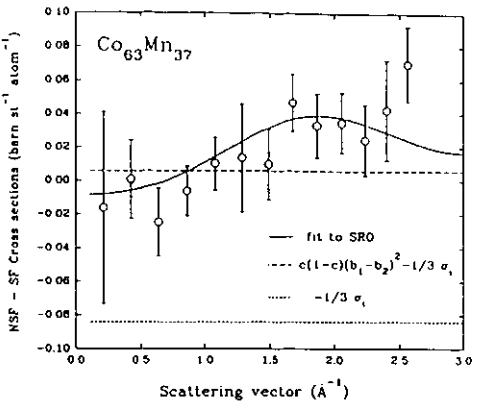

Figure 2. The plot of $\sigma_{nsf} - \sigma_{sf}$ for $Co_{63}Mn_{37}$ showing the values of the incoherent cross sections (Sears 1984), and the fit to the data of the atomic short-range order function.

Table 1. Cowley short-range-order parameters for the two samples examined.

$Co_{63}Mn_{37}$	Cowley parameter	Standard deviation
α_0	0.026	0.006
α_1	−0.005	0.001
α_2	0.004	0.004
$Co_{68}Mn_{32}$	Cowley parameter	Standard deviation
α_0	0.03	0.02
α_1	−0.020	0.005
α_2	0.00	0.01

It is worth nothing here that the fitted data contain not only the atomic disorder cross section, but also $-\frac{1}{3}$ times the nuclear spin incoherent cross section, and this is why the values are negative for small scattering vectors. Parameters for further neighbours were progressively added to the fitting expression and the fitted parameters checked for error and interdependence. χ^2 was calculated for each fitted expression and it was noted that the addition of terms to the expression beyond that for second neighbour resulted in only a marginal improvement in χ^2. At the same time, the further parameters were grossly uncertain and interdependent. We are thus confident that within the uncertainties stated in table 1 all fitted parameters are significant. The scattering-vector-independent cross section α_0 should be

$$\alpha_0 = 1 - \frac{\sigma_i}{12\pi c(1-c)(b_{Co} - b_{Mn})^2}$$

where σ_i is the average total nuclear spin incoherent cross section for the two species and the bs are the scattering lengths. Using the tabulated values (Sears 1984) gives the line in figure 2, and the value for α_0 of 0.07 ± 0.08 b sr^{-1}/atom compares well with the fitted value of α_0 further confirming the significance of the fit.

Any dependence of the magnetic cross section can then be isolated by subtracting the cross section in figure 2 from the total cross section. The cross section thus isolated contains the magnetic plus $\frac{4}{3}$ times the nuclear spin incoherent cross section. Rather than subtract the individual points we have subtracted the fit detailed above so that any variation of the magnetic cross section can be more easily seen (see figure 3).

The remaining contribution to this cross section, 4/3 times the nuclear spin incoherent cross section, is marked by the horizontal dashed line. Ideally, this should represent the minimum value that this cross section can have. In the plots some points fall below this lower limit. This is due to the uncertainty in calculating the absolute cross sections of the data, and is no reflection of the features of the data, which we believe to be real. The errors shown on our points are the combination of the counting errors from the specimen and from the vanadium standard. Inclusion of density errors, errors in attenuation and multiple-scattering corrections would increase these errors to about 5% of the cross section shown. In addition, the errors quoted for the standard values of spin incoherent cross sections of the two constituents are about 5%.

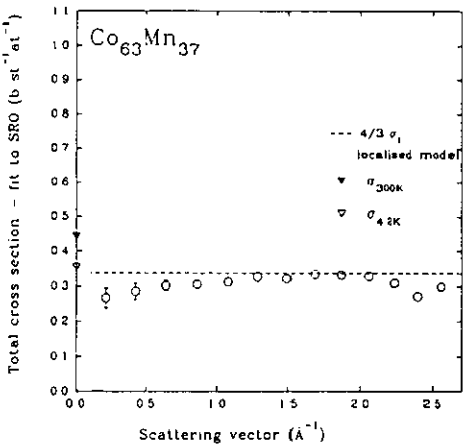

Figure 3. The plot for $Co_{63}Mn_{37}$ of the total cross section minus the fit to the atomic short-range order, leaving an effective cross section of $\frac{4}{3}\sigma_i + \sigma_m$. The neutron cross section at $\kappa = 0$ as calculated from the susceptibility data at temperatures 4.2 and 300 K have been included (Kouvel 1960). Also marked is the expected cross section at 300 K using the mean atomic moments as calculted by Koucel from the high-temperature Curie constant.

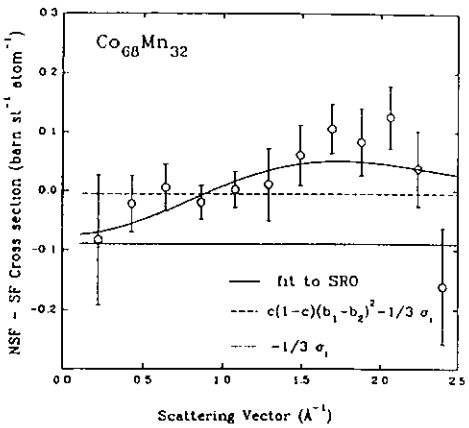

Figure 4. The plot of $\sigma_{nsf} - \sigma_{sf}$ for $Co_{68}Mn_{32}$ showing the values of the incoherent cross sections (Sears 1984), and the fit to the data of the atomic short-range-order function.

Values for the neutron cross section at $\kappa = 0$ can be estimated from susceptibility data of Kouvel (1960). If the scattering is quasielastic, the real part of the susceptibility can be used to calculate the cross section according to the equation

$$\frac{d\sigma}{d\Omega} = \left(\frac{e\gamma}{\hbar c}\right)^2 \frac{k_B T}{\rho} \chi(\kappa)$$

where ρ is the atomic density. For this approximation to be valid the incident and scattered wavevector magnitudes need to be closely similar and the energy width of the scattering should be much less than $k_B T$. The magnetic cross section in these alloys is much smaller than nuclear contributions but the time-of-flight spectra taken show the scattering confined within an FWHM of 0.5 meV with an incident neutron energy of 6 meV. $\kappa = 0$ points extracted from Kouvel's data at 4.2 and 300 K are shown in figure 3 added to the theoretical value for the nuclear spin incoherent cross section. They are consistent with a small magnetic cross section of the same order of magnitude as that which could be inferred from the experimental results considering the experimental absolute uncertainty of about 5%.

The data in figure 3 are very different from the cross section which would be expected if the average paramagnetic moment were that determined from the Curie constant by Kouvel and localized on each atom. The form of this cross section with first-neighbour correlations only is

$$\frac{d\sigma}{d\Omega} = \tfrac{2}{3}(e^2/2mc^2)^2 f^2(\kappa) g^2 \bar{S}(\bar{S}+1)\{1 + 12\gamma_1[\bar{S}^2/\bar{S}(\bar{S}+1)](\sin \kappa R_1/\kappa R_1)\}$$

with a spin $\bar{S}$ on every site. When the value of $\bar{S}$ is that obtained from the Curie constant measured by Kouvel, and the value of the first-neighbour spin correlation γ_1 is obtained from the value of the cross section in the forward direction also coming from the 300 K susceptibility, the cross section has a scattering vector dependence as shown in figure 3. It is clear that the atomic moments are nowhere near those required to explain the susceptibilty in a Curie–Weiss manner. Nevertheless a small maximum can be observed in the experimental results indicative of antiferromagnetic first-neighbour correlations. This was also observed by Men'shikov *et al* (1985) but from this study it is clear that at least some of the broad maximum observed by Men'shikov and his colleagues is due to atomic short-range order.

The same technique was used to fit the atomic short-range order in $Co_{68}Mn_{32}$. The Cowley parameters are shown in table 1 and are rather larger than those for the other alloy. This may be due to a tendency for the alloy system to order as Co_3Mn in the normal FCC manner (e.g. Ni_3Mn). Again there is reasonable agreement between the fitted α_0 and that calculated from the two scattering lengths and the nuclear spin incoherent cross sections (-0.07 ± 0.08 b sr^{-1}/atom). The fit is shown in figure 4 and, as for the other alloy, it was subtracted from the total cross section to isolate the κ dependence of the magnetic cross section. The result is shown in figure 5 along with the calculated value of $\frac{4}{3}\sigma_i$. The same uncertainties in the absolute cross section are present in these data but there is more relative uncertainty because the results consist of data from only one temperature.

Estimates of the $\kappa = 0$ cross section have been made from the results of Kouvel. If the upturn of the neutron cross section at low κ is to be believed there is agreement with the 300 K point from the susceptibility. The point from the susceptibility at 4.2 K is somewhat lower but this might be because the alloy is magnetically glassy at this temperature and its full susceptibility is not observed at normal laboratory times. The most important point is that again the magnetic response of this alloy is not from individual localized moments but from large moment clouds encompassing many atoms. Depending on the lowest κ point the clouds could have an extent of 20 Å or more. In fact the shape of the scattering is similar to that measured for $Co_{75}Mn_{25}$ by Cable (1982) in the ferromagnetic phase. Hicks *et al* (1969) could describe the distribution of ferromagnetic Ni–Cu alloys close to the critical concentration for

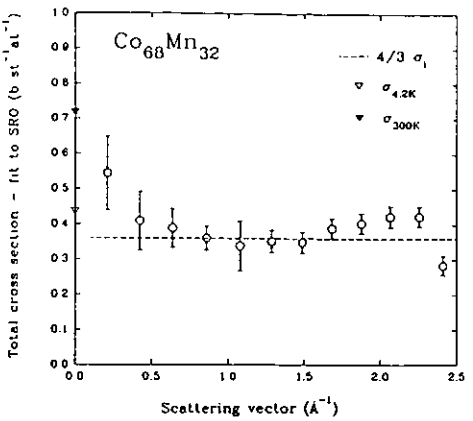

Figure 5. The plot for $Co_{68}Mn_{32}$ of the total cross section minus the fit to the atomic short-range order, leaving an effective cross section of $\frac{4}{3}\sigma_i + \sigma_m$. The neutron cross sections at $\kappa = 0$ as calculated from the susceptibility data at temperatures 4.2 and 300 K have been included (Kouvel 1960).

ferromagnetism in terms of the superposition of clouds of moment. This might be what is observed in the Co–Mn system both sides of the critical concentration. In this particular alloy the clouds would be paramagnetic or superparamagnetic and frozen at low temperatures.

There are therefore only small moments on individual atoms in the concentration range between ferromagnetism and antiferromagnetism in the Co-Mn system. This result was foreshadowed by Cable (1982) when he found that the average moment on Mn in ferromagnetic Co was $\sim 0.3\ \mu_B$ with very little fluctuation with environment and that the ferromagnetic average moments on the two species decreased with the addition of Mn. What we have found here is the logical end of such a trend.

5. Conclusion

Investigation of the short-range order in $Co_{63}Mn_{37}$ and $Co_{68}Mn_{32}$ revealed a peak in the atomic short-range order round the (100) position of the FCC structure, with some similar structure in the magnetic short-range order only for the $Co_{63}Mn_{37}$. The data, while following the trend discovered by Cable (1982) and Kouvel (1960), showing a steadily decreasing ferromagnetic moment with increasing Mn concentration, also appear to contradict the findings of Kouvel (1960) directly with regards to a steadily increasing atomic paramagnetic moment with increasing Mn concentration. This suggests an actual change in the intrinsic moment of the atoms, with large magnetic susceptibilities being given by relatively large-scale cooperation between the small local moments.

Acknowledgments

The authors are very grateful to Dr E Gray for making the samples, Mr R Liebach and Mr R Mackie for their assistance in structure and composition determination,

and Dr R L Davis for his helpful and encouraging comments. This experiment was completed with the financial assistance of AINSE and ARC. A R Wildes receives a Monash Physics Department Scholarship.

References

Bally D, Gheorghiu Z and Păsculescu D 1964 *Acta Crystallogr.* **17** 1529
Blech I A and Averbach B L 1965 *Phys. Rev.* A **137** 1113
Cable J W 1982 *Phys. Rev.* B **25** 4670
Cussen L D, Osborn J C, Gibbs P and Hicks T J 1992 *Nucl. Instrum. Methods* A **314** 155
Harders T M, Hicks T J and Wells P 1985 *J. Appl. Crystallogr.* **18** 131
Hicks T J, Rainford B D, Kouvel J S, Low G G and Comly J 1969 *Phys. Rev. Lett.* **22** 531
Kouvel J S 1960 *J. Phys. Chem. Solids* **16** 107
Marshall W 1968 *J. Phys. C: Solid State Phys.* **1** 88
Men'shikov A Z, Takzei G A, Dorofeev Yu A, Karantsev V A, Kotstyshin A K and Sych I I 1985 *Sov. Phys.–JETP* **62** 734
Rhiger D R, Müller D and Beck P A 1980 *J. Magn. Magn. Mater.* **15–18** 165
Sears V F 1984 Thermal neutron scattering lengths and cross sections for condensed matter research *AECL Report* 8490